

Droop-Controlled Inverters are Kuramoto Oscillators^{*}

John W. Simpson-Porco Florian Dörfler Francesco Bullo^{*}

^{*} Center for Control, Dynamical Systems, and Computation, University of California, Santa Barbara, Santa Barbara, CA 93106, USA, (e-mail: {johnwsimpsonporco,dorfler,bullo}@engineering.ucsb.edu)

Abstract: Motivated by the recent interest in smart grid technology and by the push towards distributed and renewable energy, we study the parallel operation of DC/AC inverters in a lossless microgrid. We show that the parallel interconnection of DC/AC inverters equipped with conventional droop controllers is precisely described by the Kuramoto model of coupled phase oscillators. This novel description, together with results from the theory of coupled oscillators, allows us to characterize the behavior of the network of inverters. Specifically, we provide a necessary and sufficient condition for the existence of a synchronized solution that is unique and exponentially stable. Remarkably, we find that the existence of such a synchronized solution does not depend on the selection of droop coefficients. We prove that the inverters share the network power demand in proportion to their power ratings if and only if the droop coefficients are selected proportionally, and we characterize the set of feasible loads which can be serviced. These results hold without assumptions on identical line characteristics or voltage magnitudes.

Keywords: Inverters; Power-system control; Smart power applications; Synchronization; Distributed control; Oscillators; Electric power systems; Load flow solutions;

1. INTRODUCTION

Microgrids appear to be the most natural extension of classical energy generation to a renewable and distributed setting. A *microgrid* is a low-voltage electrical network, heterogeneously composed of distributed generation, storage, load, and managed autonomously from the larger primary network. Microgrids are able to connect to the wide area electric power system (WAEPS) through a Point of Common Coupling (PCC), but are also able to “island” themselves and operate independently. Energy generation within a microgrid can be highly heterogeneous, combining photovoltaic farms, wind turbines, thermo-solar power, biomass, geothermal, and gas micro-turbines. Many of these devices generate either variable frequency AC power or DC power, and are therefore interfaced with a synchronous AC microgrid via power electronic devices called DC/AC *power converters*, or simply *inverters*. In islanded operation, inverters are operated as *voltage sourced inverters* (VSIs), which act much like ideal voltage sources. It is through these VSIs that actions must be taken to ensure synchronization, security, power balance and load sharing in the network.

Literature Review: A primary topic of interest within the microgrid community is the problem of accurately sharing both active and reactive power among a bank of inverters operated *in parallel*. Such a network is depicted in Figure 1, in which each inverter transmits power directly to the

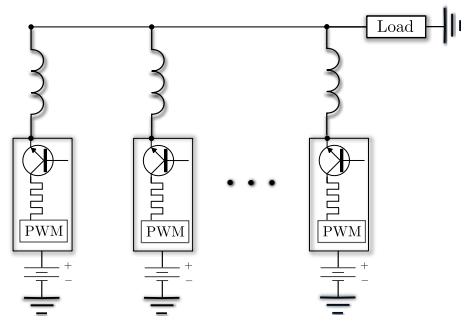


Fig. 1. Schematic of inverters operating in parallel in a microgrid. The horizontal line is a single electrical node. The inverters convert the externally supplied DC power to AC power in order to satisfy the power demand at the load.

load. As detailed in a recent review (Mohd et al., 2010), power sharing techniques generally fall into three categories, namely master/slave, current sharing, and “droop” methods. The first two methods unfortunately require some form of on-line global communication among the units, and introduce a common failure point for the entire system. This lack of redundancy and need for communication makes these techniques undesirable in a truly distributed “plug and play” setting.

The droop controllers however do not require explicit communication between inverter units during operation. The original reference for this methodology appears to be (Chandorkar et al., 1993), where Chandorkar *et al.* introduce what we will refer to as the *conventional droop controller*. The conventional droop controller is a heuristic

^{*} This work was supported in part by the National Science Foundation NSF CNS-1135819 and by National Science and Engineering Research Council of Canada. Extended version available at (Simpson-Porco et al., 2012).

based on physical intuition gleaned from the study of high-voltage WAEPS, and at its core relies on the decoupling of active and reactive power for small power angles and non-mixed line conditions.

It is well known that for lossless lines and small power angles, active power flows are controlled by the voltage power angles. In this case, the droop method attempts to emulate the behavior of a classical synchronous generator by imposing an inverse relation at each inverter between frequency and active power injection (Kundur, 1994). Under other network conditions, the method takes different forms (Yao et al., 2011). Some representative references for the basic methodology are Tuladhar et al. (1997); Lopes et al. (2006); Li and Kao (2009) and Guerrero et al. (2009). Small-signal stability analyses are presented under various assumptions in Marwali et al. (2007); Mohamed and El-Saadany (2008); Majumder et al. (2009) and the references therein. The recent work by Zhong highlights many of the drawbacks of the conventional droop method (Zhong, 2013).

Another set of literature relevant to our investigation is that pertaining to synchronization of coupled oscillators, in particular the classic *Kuramoto model* introduced in (Kuramoto, 1975). A generalization of this model considers $n \geq 2$ coupled oscillators, each represented by a phase $\theta_i \in \mathbb{S}^1$ (the unit circle) and a natural frequency $\omega_i \in \mathbb{R}$. The system of coupled oscillators obeys the dynamics

$$\dot{\theta}_i = \omega_i - \sum_{j=1}^n a_{ij} \sin(\theta_i - \theta_j), \quad i \in \{1, \dots, n\}, \quad (1)$$

where $a_{ij} \geq 0$ is the coupling strength between the oscillators i and j . The model can be visualized as n kinematic particles, each rotating on the unit circle at frequency ω_i , and connected together by linear springs. The literature on Kuramoto oscillators is vast, and the model has attracted tremendous interest from the physics, control, dynamical systems, and neuroscience communities. See the recent work (Dörfler and Bullo, 2011) and references therein.

Review of Frequency-Droop Method: The *frequency-droop method* is the foundational technique for inverter control to ensure that the *active power* demand at the load is shared among a bank of parallel VSIs, in proportion to their power ratings. In case of inductive output impedance, the controller specifies an instantaneous change in the frequency ω_i of the voltage signal at the i^{th} inverter according to

$$\omega_i = \omega^* - n_i(P_{e,i} - P_i^*), \quad i \in \{1, \dots, n\}, \quad (2)$$

where ω^* is a rated frequency, $P_{e,i}$ is the active electrical power injection at bus i , and P_i^* is the nominal active power injection when operated at the rated frequency. The parameter $n_i > 0$ is referred to as the *droop coefficient*. It is clear from (2) that for $P_{e,i} \neq P_i^*$, the operating frequency of the i^{th} inverter deviates from its nominal rated frequency.

Limitations of the Literature: Despite forming the foundation for the operation of parallel VSIs, the droop control law (2) has never been subject to a full nonlinear analysis (Zhong, 2013). To the authors' knowledge, no conditions have ever been presented under which the closed-loop system (2) possess a synchronous steady state, nor have

any statements been made about the convergence rate to such a steady state should one exist. Stability results that are presented rely on analysis of a linearized model, and sometimes come packaged with assumptions involving certain admittances in the system being small compared to others. Stability and power sharing results are typically presented for the case of two inverters, with the corresponding generalized calculation to larger networks left implicit or unclear. No analytic guarantees are given in terms of performance.

Contributions: The contributions of this paper are as follows. We begin with our key observation that the nonlinear differential equations governing the closed-loop system of a microgrid under the frequency-droop controller can be equivalently rewritten as a non-uniform multi-rate Kuramoto model of first-order phase-coupled oscillators. This insight allows us to give several interesting interpretations of the resulting feedback interconnection. We present a necessary and sufficient condition for the existence of a locally exponentially stable and synchronized solution of the closed-loop, and provide an explicit bound on the exponential convergence rate. In particular, we show that the method is stabilizing independent of the droop coefficient values, and that the steady state solution is unique and locally exponentially stable. In comparison to the existing literature, we show that if the droop coefficients are selected in proportion to the rated power values, the inverters share power proportionally without assumptions on large output impedances or identical voltage magnitudes.

Paper Organization: The remainder of this section introduces some notation and reviews some fundamental material from algebraic graph theory, power systems and coupled oscillator theory. In Section 2 we motivate the mathematical models used throughout the rest of the work, discussing both inverter and network modeling. In Section 3 we perform a full nonlinear stability analysis of the conventional frequency-droop method, and present the results described in the contributions section above.

Sets, vectors and functions: Given a finite set \mathcal{V} , let $|\mathcal{V}|$ denote its cardinality. Given an n -tuple (x_1, \dots, x_n) , let $x \in \mathbb{R}^n$ be the associated vector. For a real valued 1D-array $\{x_i\}_{i=1}^n$, we let $\text{diag}(\{x_i\}_{i=1}^n)$ be the associated diagonal matrix. We denote the $n \times n$ identity matrix by I_n . Let $\mathbf{1}_n$ and $\mathbf{0}_n$ be the n -dimensional vectors of all ones and all zeros. For a vector $x \in \mathbb{R}^n$, we define $\mathbf{sin}(x) \triangleq (\sin(x_1), \dots, \sin(x_n))^T \in \mathbb{R}^n$.

Algebraic graph theory: A weighted graph G without self-loops is a triple $G = (\mathcal{V}, \mathcal{E}, L)$ where \mathcal{V} is a set of nodes, $\mathcal{E} \subseteq \mathcal{V} \times \mathcal{V}$ is a set of edges, and $L \in \mathbb{C}^{|\mathcal{V}| \times |\mathcal{V}|}$ is the *Laplacian matrix* of the graph. If a number $\ell \in \{1, \dots, |\mathcal{E}|\}$ and an arbitrary direction is assigned to each edge $(i, j) \in \mathcal{E}$, the *oriented node-edge incidence matrix* $B \in \mathbb{R}^{|\mathcal{V}| \times |\mathcal{E}|}$ is defined component-wise as $B_{k\ell} = 1$ if node k is the sink node of edge ℓ and as $B_{k\ell} = -1$ if node k is the source node of edge ℓ , with all other elements being zero. For $x \in \mathbb{R}^n$, $B^T x$ is the vector with components $x_i - x_j$, with $(i, j) \in \mathcal{E}$. If $\text{diag}(\{a_{ij}\}_{(i,j) \in \mathcal{E}})$ is the diagonal matrix of edge weights, then $L = B \text{diag}(\{a_{ij}\}_{(i,j) \in \mathcal{E}}) B^T$. If the graph is connected, then $\ker(B^T) = \ker(L) = \text{span}(\mathbf{1}_n)$.

Moreover, L is positive semidefinite, with eigenvalues $\lambda_j(L)$, $j \in \{1, \dots, |\mathcal{V}|\}$, which can be ordered as $0 = \lambda_1(L) < \lambda_2(L) \leq \dots \leq \lambda_{|\mathcal{V}|}(L)$. We will briefly make use of the *Moore-Penrose inverse* L^\dagger of the Laplacian matrix L .

Geometry on the n -torus: An *angle* is a point $\theta \in \mathbb{S}^1$, and an *arc* is a connected subset of \mathbb{S}^1 . With a slight abuse of notation, let $|\theta_1 - \theta_2|$ denote the *geodesic distance* between two angles $\theta_1, \theta_2 \in \mathbb{S}^1$. The n -torus $\mathbb{T}^n = \mathbb{S}^1 \times \dots \times \mathbb{S}^1$ is the Cartesian product of n unit circles. For $\gamma \in [0, \pi/2)$ and a given graph $G = (\mathcal{V}, \mathcal{E}, \cdot)$, let $\overline{\Delta}_G(\gamma) = \{\theta \in \mathbb{T}^{|\mathcal{V}|} : \max_{\{i,j\} \in \mathcal{E}} |\theta_i - \theta_j| \leq \gamma\}$ be the closed set of angle arrays $\theta = (\theta_1, \dots, \theta_n)$ with neighboring angles θ_i and θ_j , $\{i, j\} \in \mathcal{E}$ no further than γ apart.

Power flow equation: Consider a lossless, synchronous AC electrical network with n nodes, purely inductive admittance matrix $Y \in \mathbb{C}^{n \times n}$, nodal voltage magnitudes $E_i > 0$, and nodal voltage phase angles $\theta_i \in \mathbb{S}^1$. The active electrical power $P_{e,i} \in \mathbb{R}$ injected into the network at node i is given by (Kundur, 1994)

$$P_{e,i} = \sum_{j=1}^n E_i E_j |Y_{ij}| \sin(\theta_i - \theta_j), \quad i \in \{1, \dots, n\}. \quad (3)$$

Synchronization: Consider the first order phase-coupled oscillator model (1) defined on a graph $G = (\mathcal{V}, \mathcal{E}, L)$. A solution $\theta : \mathbb{R}_{\geq 0} \rightarrow \mathbb{T}^{|\mathcal{V}|}$ of (1) is said to be *synchronized* if (a) there exists a constant $\omega_{\text{sync}} \in \mathbb{R}$ such that for each $t \geq 0$, $\dot{\theta}(t) = \omega_{\text{sync}} \mathbf{1}_{|\mathcal{V}|}$ and (b) there exists a $\gamma \in [0, \pi/2)$ such that $\theta(t) \in \overline{\Delta}_G(\gamma)$ for each $t \geq 0$. That is, every oscillator rotates at the constant speed ω_{sync} , with all pairwise geodesic distances *along edges* less than or equal to γ .

2. PROBLEM SETUP FOR MICROGRID ANALYSIS

Inverter Modeling: DC/AC inverters are power electronic devices with complex nonlinear characteristics. A DC source is connected to the input of a bridge circuit consisting of insulated gate bipolar transistors (IGBTs) arranged as switches, with an externally applied pulse-width modulation (PWM) signal being used to control the voltage level at the output of the inverter bridge. If the PWM switching frequency is chosen much faster than the frequency of the desired output signal, the switched signal averages locally to the desired reference signal. The end result is that an inverter can be modeled to a good approximation as a controlled voltage source behind a reactance, an approximation which is standard in the microgrid literature. Further modeling explanation can be found in (Furtado et al., 2008; Weiss et al., 2004; ?) and the references therein.

Islanded Microgrid Modeling: A mathematical model of a parallel microgrid is that of a weighted graph $G = (\mathcal{V}, \mathcal{E}, Y)$, where $\mathcal{V} = \{v_0, \dots, v_n\}$ is the set of nodes, \mathcal{E} is the set of edges, and $Y \in \mathbb{C}^{(n+1) \times (n+1)}$ is the bus admittance matrix of the network. We let nodes $1, \dots, n$ correspond to the inverter connection points, and let the 0^{th} node be the load point. With this, the node-edge incidence matrix of G has the simple form

$$B = [-\mathbf{1}_n \ I_n]^T. \quad (4)$$

For $i \in \{1, \dots, n\}$, $\sqrt{-1} \cdot b_{i0}$ is the admittance of the edge between the inverter i and the load. The output impedance of the inverter can be controlled to be purely

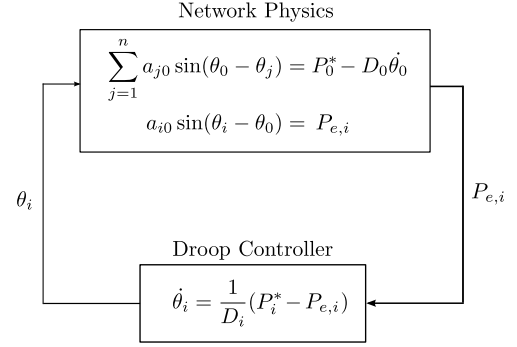


Fig. 2. Feedback loop for the frequency-droop controller.

imaginary, and we absorb its value into the line susceptance $b_{i0} < 0$. The network admittance matrix Y is then given by $Y = \sqrt{-1} \cdot B \text{diag}(\{b_{i0}\}_{i=1}^n) B^T$. To the i^{th} node we assign a voltage signal of the form $E_i(t) = E_i \cos(\omega_0 t + \theta_i)$, where $\omega_0 > 0$ is the nominal angular frequency, $E_i > 0$ is the RMS voltage, and $\theta_i \in \mathbb{S}^1$ is the voltage phase angle. From the load flow equations (3), the i^{th} inverter therefore injects a time-averaged real power $P_{e,i} = E_i E_0 |Y_{i0}| \sin(\theta_i - \theta_0)$. We will assume this value is restricted to the interval $[0, \overline{P}_i]$ where $\overline{P}_i < E_i E_0 |Y_{i0}|$ is the *rating* of inverter i .

3. NONLINEAR ANALYSIS OF FREQUENCY DROOP CONTROL

We now connect the frequency-droop method (2) to a network of first-order phase-coupled oscillators akin to (1). In what follows we restrict our attention to the analysis of active power flows, and assume the voltage magnitudes at each bus to be fixed, but not necessarily identical. We consider the problem of stable operation and proportional active power sharing among n paralleled inverters in a lossless, islanded microgrid. We assume that each inverter has precise measurements of its time-averaged active power injection $P_{e,i}$.

An equivalent reformulation of the droop controller (2) at inverter $i \in \{1, \dots, n\}$ is given by

$$D_i \dot{\theta}_i = P_i^* - P_{e,i}. \quad (5)$$

The controller (5) is a rewriting of the droop controller (2), with $\omega_i = \omega_0 + \dot{\theta}_i$, $n_i = D_i^{-1}$, and $\omega^* = \omega_0$. Using the active load flow equations (3), we obtain

$$D_i \dot{\theta}_i = P_i^* - E_i E_0 |Y_{i0}| \sin(\theta_i - \theta_0), \quad i \in \{1, \dots, n\}. \quad (6)$$

For a constant power load $P_0^* < 0$ we must also satisfy the (lossless) power balance equation

$$0 = P_0^* + \sum_{i=1}^n P_{e,i} = P_0^* + \sum_{i=1}^n E_i E_0 |Y_{i0}| \sin(\theta_i - \theta_0). \quad (7)$$

The proposed feedback scheme is illustrated in Figure 2. Augmenting the power balance (7) with an additional frequency-dependent load $D_0 \dot{\theta}_0$, the closed-loop frequency-droop controlled system (6)–(7) is seen to be in exact correspondence with a network of *multi-rate Kuramoto oscillators* similar to those described in (1). The prefix “multi-rate” refers to the heterogeneous time constants D_i which regulate the individual speeds of the oscillators. One can interpret the constant power load case of (7) with $D_0 = 0$ as the limit of the phase oscillator at the load becoming extremely fast as $D_0 \rightarrow 0^+$ (Sastry and Varaiya,

1980). We summarize the above discussion in Theorem 1, the proof of which is immediate. From now on we will for simplicity write $a_{i0} \triangleq E_i E_0 |Y_{i0}|$.

Theorem 1. (Droop-controlled inverters are Kuramoto oscillators) Consider the parallel microgrid depicted in Figure 1. The following two statements are equivalent:

- (i) each inverter is controlled according to the frequency-droop method (5) and the electrical network obeys the active power flow equations (3);
- (ii) the closed-loop system is a network of multi-rate Kuramoto oscillators described by (6)–(7), with rate constants D_i , natural frequencies P_i^* and coupling weights a_{i0} .

Remark 2. (Interpretation of frequency-droop controller) There are two insightful ways to interpret the action of the control law.

- (i) Figure 2 suggests the following interpretation; the controller modifies the phase angle at each inverter according to whether the nominal power value P_i^* balances the active power demand $P_{e,i}$ or not. The hope is then that the state $\theta \in \mathbb{T}^{n+1}$ evolves towards a stable root of the power flow equations (3). The method therefore specifies a continuous version of the Newton-Raphson iteration (c.f. dynamic optimization).
- (ii) A rearrangement of the droop controller (5) shows that the controller specifies the total power injection at each inverter as the sum of a constant power injection P_i^* and a frequency dependent power injection $-D_i \dot{\theta}_i$. It is this frequency-dependent term which specifies the difference in power between the nominal and necessary power injections. The controller is therefore a structure preserving controller, in the sense of Bergen and Hill (1981).

A natural question now arises: under what conditions on the power injections, network admittances, and droop coefficients does the closed-loop system (6)–(7) possess a stable, synchronous solution? The following result provides a definitive answer and characterizes some important properties of the solution.

Theorem 3. (Existence and Stability of Sync'd Solution) Consider the frequency-droop controlled system (6)–(7), and define the scaled power imbalance ω_{avg} by $\omega_{\text{avg}} \triangleq (\sum_{i=0}^n P_i^*) / (\sum_{i=1}^n D_i) \in \mathbb{R}$. The following two statements are equivalent:

- (i) **Synchronization:** There exists a $\gamma \in [0, \pi/2)$ such that the closed-loop system (6)–(7) possess a locally exponentially stable and unique synchronized solution $t \mapsto \theta^*(t) \in \overline{\Delta}_G(\gamma)$ for all $t \geq 0$;
- (ii) **Parametric condition:**

$$\Gamma \triangleq \max_{i \in \{1, \dots, n\}} |(P_i^* - \omega_{\text{avg}} D_i) / a_{i0}| < 1. \quad (8)$$

If the equivalent statements (i) and (ii) hold true, then the quantities Γ and $\gamma \in [0, \pi/2)$ are related uniquely via $\Gamma = \sin(\gamma)$, and following statements hold:

- a) **Explicit synchronized solution and frequency:** The synchronized solution satisfies $\theta^*(t) =$

$(\theta_0 + \omega_{\text{sync}} t \mathbf{1}_{n+1}) \pmod{2\pi}$ for some $\theta_0 \in \overline{\Delta}_G(\gamma)$, where $\omega_{\text{sync}} = \omega_{\text{avg}}$, and the synchronized angular differences satisfy $\sin(\theta_i^* - \theta_0^*) = (P_i^* - \omega_{\text{sync}} D_i) / a_{i0}$, $i \in \{1, \dots, n\}$;

- b) **Explicit synchronization rate:** The local exponential synchronization rate is no worse than

$$\lambda \triangleq \frac{\lambda_2(L)}{\max\{D_1, \dots, D_n\}} \sqrt{1 - \Gamma^2}, \quad (9)$$

where L is the Laplacian matrix with weights $\{a_{i0}\}_{i=1}^n$ and node-edge incidence matrix B given by (4).

Remark 4. (Physical interpretation and comments) Physically, the parametric condition (8) states that the active power injection at each inverter be feasible. In this sense, the stability of the overall system decouples into the stability of individual inverters. In the proof we show that without loss of generality, we can place ourselves in an appropriate rotating frame in which the necessary and sufficient condition (ii) reads that $\max_{i \in \{1, \dots, n\}} |\tilde{P}_i / a_{i0}| < 1$, for some appropriately defined values \tilde{P}_i . The **existence** of an exponentially stable synchronized solution is therefore completely independent of the selected droop coefficient values. Namely, if a synchronized solution exists for one selection of droop coefficients, a synchronized solution (albeit different) will exist for any other selection.

Proof. To begin, note that if a solution $t \mapsto \theta(t)$ to the system (6)–(7) is frequency synchronized, then by definition there exists an $\omega_{\text{sync}} \in \mathbb{R}$ such that $\dot{\theta}_i(t) = \omega_{\text{sync}}$ for each $i \in \{0, \dots, n\}$ and for all $t \geq 0$. Summing over all equations (6)–(7) then gives that $\omega_{\text{sync}} = \omega_{\text{avg}}$. It will be convenient for us to rewrite the dynamics (6)–(7) in vector notation. Letting $D \triangleq \text{diag}(0, D_1, \dots, D_n)$, $P^* \triangleq (P_0^*, P_1^*, \dots, P_n^*)^T$, for $i \in \{1, \dots, n\}$ writing $a_{i0} \triangleq E_i E_0 |Y_{i0}|$, and finally using (4) we obtain in vector form

$$D\dot{\theta} = P^* - B \text{diag}(\{a_{i0}\}_{i=1}^n) \sin(B^T \theta). \quad (10)$$

We now present a definition to facilitate the statement of our stability results. The *auxiliary system* associated to the closed-loop frequency-droop system (10) is defined by

$$D\dot{\theta} = \tilde{P} - B \text{diag}(\{a_{i0}\}_{i=1}^n) \sin(B^T \theta), \quad (11)$$

where $\tilde{P}_i = P_i^* - \omega_{\text{sync}} D_i$, $i \in \{1, \dots, n\}$ and $\tilde{P}_0 = P_0^*$. The auxiliary system has the property that $\tilde{\omega}_{\text{sync}} = \sum_{i=0}^n \tilde{P}_i / \sum_{i=1}^n D_i = 0$, and represents the dynamics (10) in a rotating frame of angular frequency ω_{sync} . Thus, frequency synchronized solutions of (10) correspond to equilibrium points of the system (11) and vice versa.

Given the Laplacian matrix $L = B \text{diag}(\{a_{i0}\}_{i=1}^n) B^T$ of the network, (11) can be equivalently rewritten in the insightful form

$$D\dot{\theta} = B \text{diag}(\{a_{i0}\}_{i=1}^n) \cdot (B^T L^\dagger \tilde{P} - \sin(B^T \theta)). \quad (12)$$

Here we have made use of the facts that $L \cdot L^\dagger = L^\dagger \cdot L = I_{n+1} - \frac{1}{n+1} \mathbf{1}_{n+1} \mathbf{1}_{n+1}^T$ (follows from the singular value decomposition (Dörfler and Bullo, 2013)) and $\mathbf{1}_{n+1}^T \tilde{P} = 0$ (due to power balancing $\sum_{i=0}^n \tilde{P}_i = 0$ in the rotating frame). For an acyclic graph, it is known (? , Theorem 3.5, (G1)) that for any $\gamma \in [0, \pi/2)$, the right-hand side of (12) admits a unique and locally exponentially stable equilib-

rium $\theta^* \in \overline{\Delta}_G(\gamma)$ if and only if $\|B^T L^\dagger \tilde{P}\|_\infty \leq \sin(\gamma)^{**}$. For the given (acyclic) star topology, direct calculation shows that the i^{th} element of the vector $B^T L^\dagger \tilde{P} \in \mathbb{R}^n$ is exactly \tilde{P}_i/a_{i0} , i.e., the ratio of the power injection at the i^{th} inverter to the maximum power transfer between the i^{th} inverter and the load. We therefore have that for any $\gamma \in [0, \pi/2)$, the necessary and sufficient condition $\|B^T L^\dagger \tilde{P}\|_\infty \leq \sin(\gamma)$ becomes $\Gamma \triangleq \max_{i \in \{1, \dots, n\}} \tilde{P}_i/a_{i0} \leq \sin(\gamma)$. Since the right-hand side of the condition $\Gamma \leq \sin(\gamma)$ is a concave and monotonically increasing function of $\gamma \in [0, \pi/2)$, there exists an equilibrium $\theta^* \in \overline{\Delta}_G(\gamma)$ for some $\gamma \in [0, \pi/2)$ if and only if the condition $\Gamma \leq \sin(\gamma)$ is true with the strict inequality sign for $\gamma = \pi/2$. This leads immediately to the condition that that $\Gamma < 1$, as claimed. Additionally, if $\Gamma = \sin(\gamma)$ for some $\gamma \in [0, \pi/2)$, then the explicit equilibrium angles are obtained from the n decoupled equations $B^T L^\dagger \tilde{P} = \mathbf{sin}(B^T \theta^*)$. In summary, the above discussion shows (in the original non-rotating coordinates) the equivalence of (i) and (ii) and statement (a).

To show statement (b), we consider the Jacobian matrix of the dynamics (11) at the exponentially stable fixed point

$$\begin{aligned} J(\theta^*) &= -D^{-1} B \text{diag}(\{a_{i0} \cos(\theta_i^* - \theta_0^*)\}_{i=1}^n) B^T \\ &= -D^{-1} L(\theta^*). \end{aligned}$$

Since $\theta^* \in \overline{\Delta}_G(\gamma)$, the matrix $L(\theta^*)$ is positive semidefinite, with a simple eigenvalue at zero corresponding to rotational invariance of the dynamics under a uniform shift of all angles. We will now bound from below the second smallest eigenvalue of $D^{-1} L(\theta^*)$, and thus give a worst case estimate of the local convergence rate of (11) to the stable equilibrium $\theta^* \in \overline{\Delta}_G(\gamma)$. A simple bound can be obtained via the *Courant-Fischer Theorem*, which states for any real symmetric matrix $M \in \mathbb{R}^{n \times n}$ that

$$\lambda_{\min}(M) = \min_{x \in \mathbb{R}^n, x \neq 0} x^T M x / x^T x.$$

To begin, for $x \in \mathbb{R}^n$ let $y = D^{-\frac{1}{2}} x$, and note that

$$y^T D^{-\frac{1}{2}} L(\theta^*) D^{-\frac{1}{2}} y / y^T y = x^T L(\theta^*) x / x^T D x.$$

Note that $y \in \mathbb{R}^n$ is an eigenvector of $D^{-\frac{1}{2}} L(\theta^*) D^{-\frac{1}{2}}$ with eigenvalue $\mu \in \mathbb{R}$ if and only if $x = D^{-\frac{1}{2}} y$ is an eigenvector of $D^{-1} L(\theta^*)$ with the same eigenvalue. Letting $y \in \mathbb{R}^n$ be an arbitrary nonzero vector in the subspace orthogonal to $\mathbf{1}_{n+1}$, we have that

$$\begin{aligned} \lambda_2(D^{-1} L(\theta^*)) &= \min_{y \in \mathbb{R}^n} y^T D^{-\frac{1}{2}} L(\theta^*) D^{-\frac{1}{2}} y / (y^T y) \\ &= \min_{x \in \mathbb{R}^n} \frac{x^T L(\theta^*) x}{x^T D x} \geq \min_{x \in \mathbb{R}^n} \frac{x^T L(\theta^*) x}{x^T x} \frac{1}{\max\{D_1, \dots, D_n\}} \\ &\geq \lambda_2(L(\theta^*)) / \max\{D_1, \dots, D_n\}. \end{aligned}$$

Since $\theta^* \in \overline{\Delta}_G(\gamma)$, the eigenvalue $\lambda_2(L(\theta^*))$ can be further bounded as $\lambda_2(L(\theta^*)) \geq \lambda_2(L) \cos(\gamma)$, where $L = B \text{diag}(\{a_{i0}\}_{i=1}^n) B^T$ is the Laplacian matrix with weights $\{a_{i0}\}_{i=1}^n$. Combining this fact with the identity $\cos(\sin^{-1}(z)) = \sqrt{1 - z^2}$ for $z \in \mathbb{R}$ suffices to show the result. \square

**The stability property proved in ?) applies, strictly speaking, only to pure ODEs. However, it is well known that a locally exponentially stable equilibrium $\theta^* \in \overline{\Delta}_G(\pi/2)$ of the DAE system (12) with $D_0 = 0$ has the same local stability properties as the identical equilibrium θ^* of the corresponding system of pure ODEs with $D_0 > 0$, see Sastry and Varaiya (1980).

3.1 Proportional Droop Coefficients and Load Sharing

Theorem 3 gives us a necessary and sufficient condition for the existence of a synchronized solution to the closed-loop system (10). However, the result offers no immediate guidance on how to properly select the droop coefficients. Indeed, we will see that an improper selection of droop coefficients can lead to behaviour which, for any choice of $P_i^* \in [0, \overline{P}_i]$, violates the actuation constraint $P_{e,i} \in [0, \overline{P}_i]$ of Section 2. We now present a definition which characterizes the ‘‘proper’’ way to select the droop coefficients. We then show that if one selects the droop coefficients in this manner, the resulting behaviour of the steady-state power flow satisfies the actuation constraints. The result also gives a bound on the magnitude of the allowable load that can be serviced without violating the power injection constraints.

Definition 5. (Proportional Droop Coefficients) The droop coefficients are said to be selected proportionally if for each $i, j \in \{1, \dots, n\}$,

$$P_i^* / D_i = P_j^* / D_j. \quad (13)$$

Lemma 6. (Power Flow Constraints & Sharing) Consider a synchronized solution the frequency-droop controlled system (6)–(7), and let the droop coefficients be selected proportionally. The following two statements are equivalent:

(i) **Power flow constraints:**

$$0 \leq P_{e,i} \leq \overline{P}_i, \quad i \in \{1, \dots, n\};$$

(ii) **Load constraints:**

$$- \left(\min_{i \in \{1, \dots, n\}} \overline{P}_i / P_i^* \right) \cdot \sum_{j=1}^n P_j^* \leq P_0^* \leq 0.$$

Moreover, the inverters share the load P_0^* proportionally according to their power ratings (i.e., $P_{e,i} / \overline{P}_i = P_{e,j} / \overline{P}_j$, $i, j \in \{1, \dots, n\}$) if and only if $P_i^* = \overline{P}_i$ for each inverter.

Proof. In synchronous steady state, we have that $\dot{\theta}_i = \omega_{\text{sync}} = (P_0^* + \sum_{i=1}^n P_i^*) / (\sum_{i=1}^n D_i)$ for each $i \in \{0, \dots, n\}$. Substituting this equality into the closed-loop (6), we see that the steady-state active power injection at each inverter is given by $P_{e,i} = a_{i0} \sin(\theta_i^* - \theta_0^*) = P_i^* - \omega_{\text{sync}} D_i$. By imposing for each $i \in \{1, \dots, n\}$ that $P_{e,i} \geq 0$, substituting the expression for ω_{sync} , and rearranging terms, we calculate for each $i \in \{1, \dots, n\}$ that

$$\begin{aligned} P_{e,i} = P_i^* - \left(\frac{P_0^* + \sum_{j=1}^n P_j^*}{\sum_{j=1}^n D_j} \right) D_i &\geq 0 \\ \iff P_0^* \leq - \sum_{j=1}^n (P_j^* - P_i^* D_j / D_i) &= 0, \end{aligned}$$

where in the final equality we have made use of the proportional selection of droop coefficients given by (13). This suffices to show that $0 \leq P_{e,i}$ for each $i \in \{1, \dots, n\}$ if and only if $P_0^* \leq 0$. If we now impose that $P_{e,i} \leq \overline{P}_i$ and again use the expression for ω_{sync} along with (13), a similar calculation to that above gives that

$$\begin{aligned} P_{e,i} \leq \overline{P}_i &\iff P_0^* \geq - \frac{\overline{P}_i}{P_i^*} \sum_{j=1}^n P_j^*, \quad i \in \{1, \dots, n\}, \\ \iff P_0^* &\geq - \left(\min_{i \in \{1, \dots, n\}} \frac{\overline{P}_i}{P_i^*} \right) \sum_{j=1}^n P_j^*, \end{aligned}$$

which shows that $P_{e,i} \leq \bar{P}_i$ for $i \in \{1, \dots, n\}$ if and only if P_0^* satisfies the above inequality. In summary, we have demonstrated two if and only if inequalities, which when taken together show the equivalence of (i) and (ii). To show the final statement, we select each P_i^* to be equal to \bar{P}_i and note that the fraction of the rated power capacity consumed by the i^{th} inverter is given by

$$\frac{P_{e,i}}{\bar{P}_i} = \frac{\bar{P}_i - \omega_{\text{sync}} D_i}{\bar{P}_i} = \frac{\bar{P}_j - \omega_{\text{sync}} D_j}{\bar{P}_j} = \frac{P_{e,j}}{\bar{P}_j},$$

for each $j \in \{1, \dots, n\}$, where we have again used (13). This completes the proof. \square

The final statement of Lemma 6 is the frequently cited *coefficient matching* condition of the microgrid/droop control literature. Note in particular that the coefficients D_i must be selected with global knowledge. The droop method therefore requires a centralized design for power sharing despite its distributed implementation, and does not allow for plug-and-play power sharing functionality without the global recomputation of all coefficients. Lemma 6 holds independent of the voltage magnitudes at each inverter, and independent of the network susceptance values.

4. CONCLUSIONS

Leveraging recent results from the theory of coupled oscillators and from classical power systems, we have presented the first nonlinear analysis of the frequency-droop controller. Works to follow will extend this analysis to reactive power sharing and to networks with non-zero transfer conductances.

REFERENCES

- Bergen, A.R. and Hill, D.J. (1981). A structure preserving model for power system stability analysis. *IEEE Transactions on Power Apparatus and Systems*, 100(1), 25–35.
- Chandorkar, M.C., Divan, D.M., and Adapa, R. (1993). Control of parallel connected inverters in standalone AC supply systems. *IEEE Transactions on Industry Applications*, 29(1), 136–143.
- Dörfler, F. and Bullo, F. (2011). On the critical coupling for Kuramoto oscillators. *SIAM Journal on Applied Dynamical Systems*, 10(3), 1070–1099.
- Dörfler, F. and Bullo, F. (2013). Kron reduction of graphs with applications to electrical networks. *IEEE Transactions on Circuits and Systems I: Regular Papers*, 60(1), 150–163. doi:10.1109/TCSI.2012.2215780.
- Furtado, E.C., Aguirre, L.A., and Tórres, L.A.B. (2008). UPS parallel balanced operation without explicit estimation of reactive power – a simpler scheme. *IEEE Transactions on Circuits and Systems II: Express Briefs*, 55(10), 1061–1065.
- Guerrero, J.M., Vasquez, J.C., Matas, J., Castilla, M., and de Vicuna, L.G. (2009). Control strategy for flexible microgrid based on parallel line-interactive UPS systems. *IEEE Transactions on Industrial Electronics*, 56(3), 726–736.
- Kundur, P. (1994). *Power System Stability and Control*. McGraw-Hill.
- Kuramoto, Y. (1975). Self-entrainment of a population of coupled non-linear oscillators. In H. Araki (ed.), *Int. Symposium on Mathematical Problems in Theoretical Physics*, volume 39 of *Lecture Notes in Physics*, 420–422. Springer.
- Li, Y.U. and Kao, C.N. (2009). An accurate power control strategy for power-electronics-interfaced distributed generation units operating in a low-voltage multibus microgrid. *IEEE Transactions on Power Electronics*, 24(12), 2977–2988.
- Lopes, J.A.P., Moreira, C.L., and Madureira, A.G. (2006). Defining control strategies for microgrids islanded operation. *IEEE Transactions on Power Systems*, 21(2), 916–924.
- Majumder, R., Ghosh, A., Ledwich, G., and Zare, F. (2009). Angle droop versus frequency droop in a voltage source converter based autonomous microgrid. In *IEEE Power & Energy Society General Meeting*, 1–8. Calgary, AB, Canada.
- Marwali, M.N., Jung, J.W., and Keyhani, A. (2007). Stability analysis of load sharing control for distributed generation systems. *IEEE Transactions on Energy Conversion*, 22(3), 737–745.
- Mohamed, Y. and El-Saadany, E.F. (2008). Adaptive decentralized droop controller to preserve power sharing stability of paralleled inverters in distributed generation microgrids. *IEEE Transactions on Power Electronics*, 23(6), 2806–2816.
- Mohd, A., Ortjohann, E., Morton, D., and Omari, O. (2010). Review of control techniques for inverters parallel operation. *Electric Power Systems Research*, 80(12), 1477–1487.
- Sastry, S. and Varaiya, P. (1980). Hierarchical stability and alert state steering control of interconnected power systems. *IEEE Transactions on Circuits and Systems*, 27(11), 1102–1112.
- Simpson-Porco, J.W., Dörfler, F., and Bullo, F. (2012). Droop-controlled inverters are Kuramoto oscillators. Available at <http://arxiv.org/abs/1206.5033>.
- Tuladhar, A., Jin, H., Unger, T., and Mauch, K. (1997). Parallel operation of single phase inverter modules with no control interconnections. In *Applied Power Electronics Conference and Exposition*, 94–100. Atlanta, GA, USA.
- Weiss, G., Zhong, Q.C., Green, T.C., and Liang, J. (2004). H^∞ repetitive control of DC-AC converters in microgrids. *IEEE Transactions on Power Electronics*, 19(1), 219–230.
- Yao, W., Chen, M., Matas, J., Guerrero, J.M., and Qian, Z.M. (2011). Design and analysis of the droop control method for parallel inverters considering the impact of the complex impedance on the power sharing. *IEEE Transactions on Industrial Electronics*, 58(2), 576–588.
- Zhong, Q.C. (2013). Robust droop controller for accurate proportional load sharing among inverters operated in parallel. *IEEE Transactions on Industrial Electronics*, 60(4), 1281–1290.